

ePathBrick: A Synthetic Biology Platform for Engineering Metabolic Pathways in *E. coli*

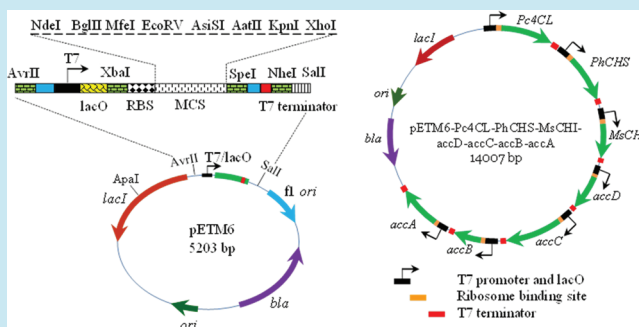
Peng Xu, Amerin Vansiri, Namita Bhan, and Mattheos A. G. Koffas*

Center for Biotechnology and Interdisciplinary Studies and Department of Chemical and Biological Engineering, Rensselaer Polytechnic Institute, Troy, New York 12180, United States

Supporting Information

ABSTRACT: Harnessing cell factories for producing biofuel and pharmaceutical molecules has stimulated efforts to develop novel synthetic biology tools customized for modular pathway engineering and optimization. Here we report the development of a set of vectors compatible with BioBrick standards and its application in metabolic engineering. The engineered ePathBrick vectors comprise four compatible restriction enzyme sites allocated on strategic positions so that different regulatory control signals can be reused and manipulation of expression cassette can be streamlined. Specifically, these vectors allow for fine-tuning gene expression by integrating multiple transcriptional activation or repression signals into the operator region. At the same time, ePathBrick vectors support the modular assembly of pathway components and combinatorial generation of pathway diversities with three distinct configurations. We also demonstrated the functionality of a seven-gene pathway (~9 Kb) assembled on one single ePathBrick vector. The ePathBrick vectors presented here provide a versatile platform for rapid design and optimization of metabolic pathways in *E. coli*.

KEYWORDS: metabolic engineering, transcriptional fine-tuning, gene assembly, pathway configuration, T7 promoter activity



As an emerging discipline, synthetic biology is becoming increasingly important to design, construct, and optimize metabolic pathways leading to desired phenotypes such as overproduction of biofuels^{1–3} and pharmaceuticals^{4,5} in genetically tractable organisms. One of the major challenges for heterologous expression of multigene pathways is to orchestrate the expression level of each of the enzymes among the selected pathways and achieve optimal catalytic efficiency. Thus, delicately designed molecular control elements have been integrated into the cell chassis to enable the host strain to precisely respond to environmental stimuli or cellular intermediates and drive carbon flux toward a target pathway. For example, engineering promoter architecture has achieved tunable gene expression in both *E. coli*⁶ and yeast⁷ at transcriptional levels; engineered metabolite-responsive riboswitches⁸ and synthetic ribosome binding sites⁹ can be used to precisely control protein expression at the translational level; metabolic flux channeling by spatial recruitment of desired metabolic enzymes at a stoichiometric ratio on a synthetic protein scaffold can efficiently prevent the loss of intermediates due to diffusion and has resulted in a 77-fold improvement in production titer.¹⁰ As witnessed by these endeavors, the advances in synthetic biology have greatly speeded up our ability to design and construct cell factories for metabolic engineering application.

To date, a number of synthetic biology approaches have been applied to metabolic pathway optimization including modification

of plasmid copy number,¹¹ promoter strength,^{12,13} and gene codon usage.¹⁴ However, most of these approaches are not modular and require time-consuming work tweaking the individual pathway components until the desired performance is achieved, which greatly compromises our ability to unlock the metabolic potential of host metabolism. From an engineering perspective, we need a more efficient approach that allows us to streamline the process of pathway construction and engineering of biological systems to be much easier and faster. Despite the availability of advanced cloning tools such as the DNA assembler,^{15,16} sequence and ligation-independent cloning (SLIC),¹⁷ and Gibson isothermal assembly,¹⁸ these tools largely rely on site-specific homologous recombination and are limited in terms of automation and the number of DNA fragments that can be assembled for pathway optimization;¹⁹ in particular, these advanced cloning tools are not amenable to very short genetic elements such as promoter, ribosome binding site, operator, and other regulatory control elements.²⁰ Hence, there exists a pressing need to develop efficient molecular assembly tools customized for metabolic pathway optimization.

Assembly of biological standard parts that conform to the BioBrick paradigm is being adopted rapidly and is becoming a standard practice in metabolic pathway engineering²¹ and

Received: March 21, 2012

Published: April 23, 2012

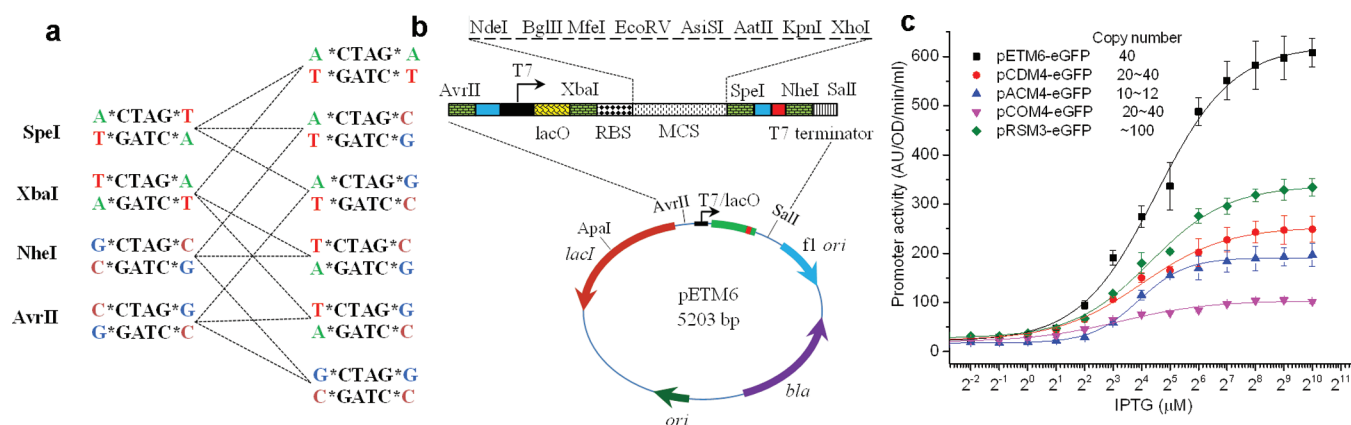


Figure 1. Basic configuration and functional analysis of the engineered ePathBrick vectors. (a) Compatible sticky ends can be generated by four isocaudamer pairs (*AvrII*, *NheI*, *SpeI*, and *XbaI*) with unique DNA recognition sequence. The resulting sticky ends can be rejoined together upon simple ligation thereby nullifying the old restriction sites. (b) The basic configuration of engineered ePathBrick vectors. (c) The dose response of promoter activity to inducer IPTG using eGFP as a reporter among the five engineered ePathBrick vectors harbored by *E. coli* BL21*(DE3) in LB media at 30 °C.

genetic circuit design.^{22,23} This technical standard was first described by Knight²⁴ and further developed by Endy and co-workers.^{25,26} The BioBrick standards take advantage of the isocaudamer pairs *XbaI* and *SpeI*, which generate compatible cohesive ends and upon ligation result in a scar sequence that cannot be cleaved by either of the original restriction enzyme pairs. Basic molecular components flanked with these isocaudamer pairs can be assembled together by iterative restriction enzyme digestion and ligation. Several groups have developed similar biological part assembly vectors (BglBricks) that utilize the *BglII* and *BamHI* compatible cohesive ends and can be used for engineering fusion proteins and expressing multiple operons from different plasmids varying in promoter strength, inducers, and plasmid copy number.^{19,27} Nevertheless, we envision that further development in synthetic biology tools for metabolic pathway engineering will depend on more efficient molecular assembly tools that support tunable gene expression, modular assembly of multi-gene pathways, and generation of pathway diversities in a combinatorial manner.

Here we present the development of a set of robust yet flexible standard vectors (so-called ePathBricks) compatible with the BioBrick standards and its application in metabolic pathway engineering. Despite sharing the same advantages as BioBrick standards (BBF RFC10) in terms of part reuse and standardization, the engineered ePathBrick vectors are designed to address several of the critical challenges faced by metabolic engineers and synthetic biologists such as lack of efficient tools for fine-tuning gene expression and construction of pathways with multiple gene components. The ePathBrick vectors feature in four isocaudamer pairs (*AvrII*, *XbaI*, *SpeI*, and *NheI*) and support the modular assembly of a number of molecular components including regulatory signal elements (promoters, operators, ribosome binding sites, and terminators) and multi-gene pathways; in addition, ePathBricks provide a platform for optimizing pathway configurations (i.e., how individual genes are connected with each other) and efficient generation of pathway diversities. To demonstrate the *in vivo* functionality and compatibility, we have successfully integrated multiple transcriptional activation and repression signals into the regulatory region of the engineered vectors. Furthermore, we have assembled and tested the production potential of a three-configuration flavonoid pathway. We show that a three-gene

flavonoid pathway can be easily diversified to 54 pathway variations through modular pathway engineering, simply by varying pathway configuration and gene order. At the end, we showcase the efficient assembly of a seven-gene heterologous pathway (around 9 Kb) on one single ePathBrick vector. The ePathBrick standard assembly method presented here allows the user to rapidly construct and optimize multigene pathways with different regulatory control elements and gene configurations as well as generation of pathway diversities.

RESULTS AND DISCUSSION

Design and Characterization of ePathBrick Vectors.

Strain development through metabolic engineering leading to biofuel and pharmaceutical molecules typically involves the manipulation of a handful of precursor or rate-limiting pathways, as illustrated in the recent example of biobutanol production from non-fermentative pathway^{28,29} and the heterologous production of taxol¹² and artemisinin³⁰ precursors in *E. coli*. One popular approach to express multigene pathways is to use the Novagen Duet vectors, which carry compatible replication origins (*ColE*, *CloDF13*, *P15A*, *CoLA*, and *RSF1030*) and independent antibiotic markers (*Am*, *Sm*, *Cm*, *Km*), allowing for effective propagation and maintenance of four plasmids and simultaneous expression of up to eight genes in a single cell.³¹ The Duet vector sets have been successfully applied to engineering a number of pathways for synthesizing hydroxybutyrate,³² biofuels,^{33,34} phenylpropanoids,^{35,36} isoprenoids,³⁷ and polyketides.³⁸ Despite these achievements, the Duet vector sets are not innate to modular pathway engineering and tunable gene expression, eclipsing its major features such as versatile plasmid copy number, broad host spectrum, as well as independent antibiotic marker. To expand its applicability in metabolic pathway engineering, we engineered the Duet vectors in order to make them conform to the basic principles of synthetic biology.

We have taken a retrosynthetic approach to design the original Duet vectors. The four isocaudamer pairs (*AvrII*, *XbaI*, *SpeI*, and *NheI*) were chosen mainly because they are compatible with the BioBrick standards, cut with high efficiency generating four letter high-affinity cohesive ends (CTAG, Figure 1a), and are rarely affected by *dam* or *dcm* methylation. (Note: only *XbaI* have *dam* overlapping methylation when TC

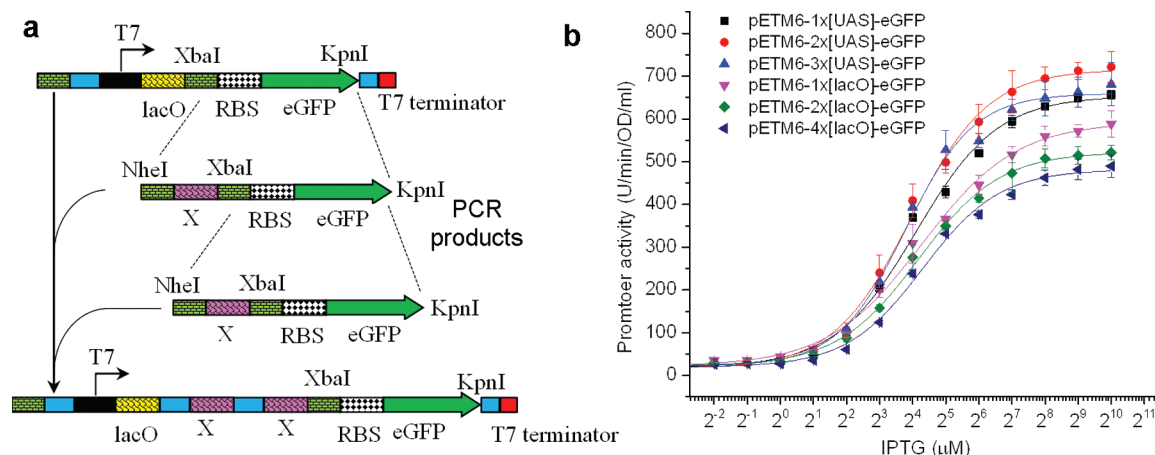


Figure 2. Fine-tuning gene expression by expanding the regulator control elements on engineered ePathBrick vectors. (a) Incorporation of repetitive tandem copies of regulatory elements (X) using *XbaI* site on ePathBrick vectors and *NheI*-flanked PCR products. The PCR product contains another *XbaI* site and can be reused for iterative integration of multiple regulatory elements on ePathBrick vectors. X is any regulatory sequence that could potentially interact with the open/closed form of promoter-RNA polymerase complex thereby activating or repressing gene expression from the downstream reporter gene. (b) Characterization of promoter activity arising from multiple copies of upstream activation sequence (UAS) and lactose repressor binding site (*lacO*) on pETM6 harbored by BL21*(DE3) growing in LB media at 30 °C.

comes with it). On the basis of the basic principles of synthetic biology,^{25,39} the four isocaudamers were arranged in such a way that the different molecular control or structural elements can be easily reused and standardized. *AvrII* was inserted upstream of the T7 promoter, *XbaI* was inserted between the operator (*lacO*) and ribosome binding site (RBS), *SpeI* was between the multiple-cloning site (MCS) and T7 terminator, and *NheI* was placed downstream of the T7 terminator. *SalI* and the native *ApaI* on the *lacI* gene was designed for easy cloning with any of the four isocaudamers. Following this principle, we have made 6, 4, 4, 4, and 3 modifications to the original pET-Duet, pCDF-Duet, pACYC-Duet, pCOLA-Duet, and pRSF-Duet vectors, respectively. The resulting vectors, pETM6, pCDM4, pACM4, pCOM4, and pRSM3 are collectively named ePathBrick vectors. A representative vector configuration is shown in Figure 1b. Detailed sequence information in Genbank format can be found in the Supporting Information (Boxes S1–S5).

To test the functionality of engineered ePathBrick vectors, enhanced fluorescence protein (eGFP) was used as a reporter and inserted at the same loci of multicloning sites among the five ePathBrick vectors to eliminate any restriction sites-associated translational inhibition.⁴⁰ We observed that green fluorescence linearly increased with time after a short time window (about 90 min) in all of the tested five constructs (Supplementary Figure S1). The rate of fluorescence change normalized with cell density and culture volume was used to characterize the promoter activity. Results shown here indicate that the dynamic range of tested promoters spanned over 3 orders of magnitude toward IPTG and the same promoter behaved distinctly in different genetic contexts (Figure 1c).

As Figure 1c shows, the saturation promoter activity in pETM6 is about 6 times stronger than that in pCOM4. The promoter activity observed in three of the ePathBrick vectors (pETM6, pCDM4, and pACM4) correlated well with their reported plasmid copy number (Figure 1c) except for pCOM4, which is not unexpected as the DNA quantity of pCOM4 isolated from an *E. coli* culture was the lowest, possibly due to the low stability of the pCOLA-derived vectors as reported by Kroll.⁴¹ Both pCOM4 and pRSM3 vectors share almost the same genetic context except for the origin of replication region,

which can account for the relatively low promoter activity in pRSM3 as the specific promoter activity (promoter activity normalized by plasmid copy number) in pRSM3 was comparable with that in pCOM4. These data suggests that all of the redesigned ePathBrick vectors are functional and the promoter activity tested in *E. coli* BL21*(DE3) is ranked in the following order: pETM6 > pRSM3 > pCDM4 > pACM4 > pCOM4. Given that one single cell is able to harbor four compatible plasmids, the broad range of promoter activity should be an invaluable tool to coordinate the expression of multigene pathways for metabolic engineering application.

Tunable Gene Expression with Expandable Regulatory Elements. Promoter architecture with defined activator or repressor binding site is directly correlated with the output of promoter activity.⁶ Thus, engineering of hybrid promoters is an effective approach to transcriptional fine-tuning with various applications, especially in the metabolic engineering area.^{7,42} Here we have developed a standardized method for modular integration of repetitive tandem copies of transcriptional activation or repression signals into the operator region of the ePathBrick vectors. Specifically, by using the isocaudamer pairs *XbaI* and *NheI*, the *NheI*-flanked PCR products can be easily incorporated into the regulatory region of the engineered ePathBrick vectors. Since the PCR products contained another *XbaI* site that can be reused, multiple copies of a regulatory signal can be integrated on the same ePathBrick vector in a tandem manner (Figure 2a), thus providing a way for modifiable transcription output.

As a case study, we chose a random upstream activation sequence (UAS)⁴³ and the native *lac* promoter repression signal (*lacO*) as a transcriptional modulator and evaluated how they impact the promoter activity. By iterative digestion and ligation, we have been able to incorporate up to three copies of UAS and four copies of repression sequence (*lacO*) into the operator region of pETM6. The time course analysis of fluorescence change (Supplementary Figure S2) demonstrated that the resulting synthetic promoters exhibited tunable activity ranging from 81% to 122% of the activities of the unmodified promoter (Figure 2b). In order to characterize the underlying mechanisms associated with promoter-RNA polymerase

Table 1. Best Fit of the Characterized Promoter Activity Using Modified Regulatory Control Elements^a

construct	P_{\min} (au)	P_{\max} (au)	K (μM)	n	R^2
pETM6-1X[UAS]-eGFP	19.42 \pm 9.53	653.54 \pm 13.32	17.20 \pm 1.38	1.17 \pm 0.10	0.9950
pETM6-2X[UAS]-eGFP	16.74 \pm 8.08	715.62 \pm 10.63	15.34 \pm 0.91	1.23 \pm 0.08	0.9971
pETM6-3X[UAS]-eGFP	21.95 \pm 8.39	659.40 \pm 10.29	13.74 \pm 0.86	1.40 \pm 0.11	0.9960
pETM6-1X[lacO]-eGFP	22.00 \pm 7.75	592.90 \pm 12.01	19.43 \pm 1.54	1.01 \pm 0.08	0.9962
pETM6-2X[lacO]-eGFP	22.49 \pm 4.91	522.55 \pm 7.03	18.11 \pm 0.96	1.17 \pm 0.07	0.9978
pETM6-4X[lacO]-eGFP	19.62 \pm 6.04	481.67 \pm 8.84	19.82 \pm 1.39	1.25 \pm 0.10	0.9958

^aData shown here indicate the simulated parameters of the Hill equation. au, arbitrary units (fluorescence unit per minute per OD per milliliter).

(RNAP) interaction, inducer and promoter input-output correlations were fitted to a phenomenological Hill equation^{44,45} of the form

$$P([I]) = P_{\min} + (P_{\max} - P_{\min}) \frac{[I]^n}{K^n + [I]^n}$$

where $[I]$ is the inducer concentration; P_{\min} is the basal level of promoter activity due to leakage; P_{\max} is the maximal promoter activity due to saturation induction; n is the Hill coefficient that determines the sensitivity (cooperativity) of repressor-promoter-RNAP interactions; and K is the apparent dissociation constant related to the half saturation concentration of inducer when promoter activity reaches half of the maximum output.

As summarized in Table 1, the half saturation constant (K value) was decreased with increasing number of upstream activation sequence (UAS) used, indicating that the incorporation of UAS into the operator region did contribute to the formation of transcriptionally competent promoter-RNAP complexes; thus the transcription output was improved compared with that of the native counterpart (native one is pETM6-1X[lacO]-eGFP in Table 1). At the same time, the promoter responded more sensitively toward IPTG, as evidenced by the Hill coefficient (n) that increased with increasing number of UAS used, suggesting increased cooperativity among the repressor-promoter-RNAP complex. When multiple copies of *lacO* were used, the half saturation constant (K) did not change while the cooperative interaction among repressor-promoter-RNAP increased (n increased), thereby resulting in more stringent control over promoter output. This data illustrates that the operator context in the engineered vectors has a profound impact on the transcription output, and the modular approach presented here can be directly translated to other ePathBrick vectors for fine-tuning gene expression.

Multigene Pathway Can Be Assembled in Three Configurations. Prokaryotic cells such as *E. coli* tend to organize metabolic enzymes in operon form, where the functionally related pathways are arranged in gene clusters and are under the control of a single regulatory signal. It is estimated that about 50% of the structural genes are organized in operon form in *E. coli*.⁴⁶ Gene cotranscription and coregulation provide an evolutionary advantage since various proteins synthesized from a single mRNA transcript could facilitate the spatial and temporal coordination of gene expression to build up multienzyme complexes often at the right subunit ratio. Using a synthetic operon comprising three fluorescence reporter genes as a model system, Lim et al. found that the expression of a given gene increased with the length of the operon, as increased transcription distance provided more time for translation to occur during transcription.⁴⁷ In terms of metabolic pathway reconstruction, a fundamental question is how individual pathways are assembled and which genetic organization or configuration is adopted for optimal pathway

output. For example, an artificial operon carrying all of the necessary genes (*atoB*, *hbd*, *crt*, *ter*, and *adhE2*) for conversion of acetyl-CoA to butanol along with the optimization of NADH driving force has led to the production of butanol at a titer of 30 g/L in *E. coli*;²⁹ heterologous production of resveratrol favored the operon configuration of two plant enzymes, *A. thaliana* 4-coumaroyl-CoA ligase and *V. vinifera* stilbene synthase, resulting in the highest resveratrol production of around 2.3 g/L in *E. coli*.⁴⁸ Hence, it is of vital importance to develop efficient tools that allow us to organize multigene pathways in different configurations, thereby possibly exploiting the full potential of cell metabolism.

Pathway configuration engineering was a built-in feature for ePathBrick vectors, where individual pathway components can be assembled and organized in three different configurations. Using a three-gene heterologous flavonoid pathway, we have been able to integrate 4-coumaroyl-CoA ligase (from *Petroselinum crispum*), chalcone synthase (from *Petunia hybrida*), and chalcone isomerase (from *Medicago sativa*) into pETM6 with three configurations by modular pathway engineering (Figure 3). Specifically, each of the pathway components can be organized either in operon (Figure 3a), pseudo-operon (Figure 3b), or monocistronic (Figure 3c) configuration using different isocaudamer pairs. The difference is that in the operon form, all of the genes were transcribed and regulated together (Figure 3a, one promoter and one terminator); in pseudo-operon form, each of the pathway genes was under the control of an independent promoter but all mRNA transcripts shared the same terminator (Figure 3b, multiple promoters but one terminator); for monocistronic form, each of the functional unit was under the control of an independent regulatory signal (Figure 3c, multiple promoters, multiple terminators).

We then tested the production potential of these three distinct flavonoid pathways in the Bl21*(DE3) strain. As shown in Figure 4, the pathway with the pseudo-operon configuration led to the highest flavonoid production of 36.7 mg/L, whereas the pathway with the operon form showed the lowest production of 1.2 mg/L, representing only 3.3% of the production obtained from the pseudo-operon form. The pathway with the monocistronic form showed slightly lower production compared with the pseudo-operon form, presumably due to the unintended interaction between the adjacent promoter and terminator. It is speculated here that the strong secondary structure (usually stem-loop hairpin structure) in the terminator region would sterically interact with the adjacent promoter and repress transcription, which is unlikely to happen in the operon or pseudo-operon configurations. Malonyl-CoA, an essential precursor in the flavonoid biosynthesis, has been proven to be a limiting factor for their production.³⁶ By overexpressing a putative four-subunit acetyl-CoA carboxylase (ACC from *P. luminescens*) to provide sufficient amount of malonyl-CoA, flavonoid production was significantly increased

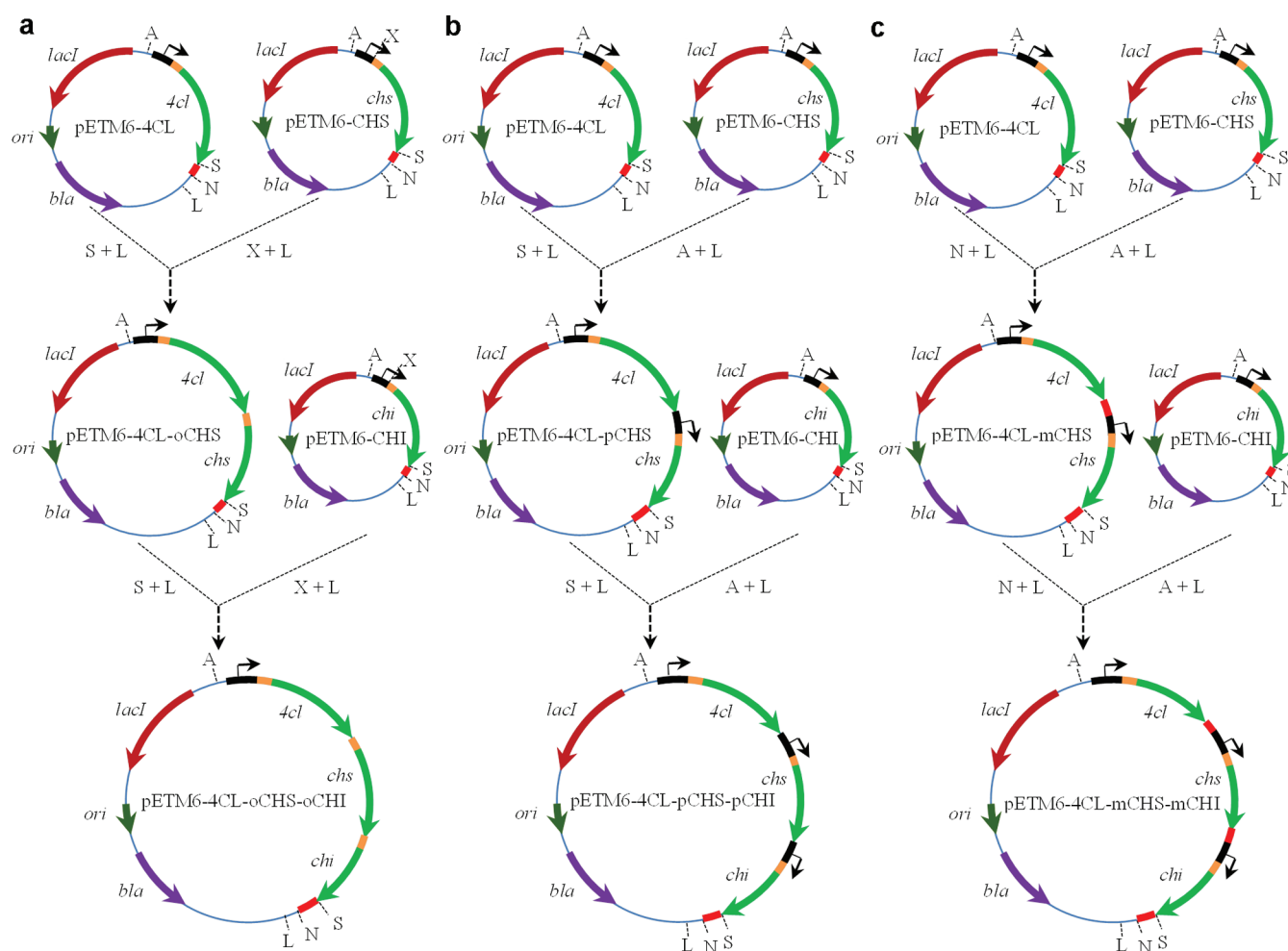


Figure 3. Easy pathway configuration engineering by modular assembly using different isocaudamer pairs. (a) A three-gene pathway was assembled in operon form, in which a cluster of genes was under the control of a single regulatory signal (one promoter, one terminator). Operon configuration can be achieved by digesting the donor vector (pETM6-CHS) with restriction enzyme pairs *Xba*I (X)/*Sal*I (L) and ligating it to the *Spe*I (S)/*Sal*I (L) digested destination vector (pETM6-4CL). *Spe*I site was retained and can be reused for iterative assembly of downstream genes. (b) A three-gene pathway was assembled in pseudo-operon or artificial operon form. Pseudo-operon configuration can be achieved by digesting the donor vector (pETM6-CHS) with restriction enzyme pairs *Avr*II (A)/*Sal*I (L) and ligating it to the *Spe*I (S)/*Sal*I (L) digested destination vector (pETM6-4CL). *Spe*I site was retained and can be reused for iterative assembly of another gene. (c) A three-gene pathway was assembled in monocistronic form. Monocistronic configuration can be achieved by digesting the donor vector (pETM6-CHS) with restriction enzyme pairs *Avr*II (A)/*Sal*I (L) and ligating it to the *Nhe*I (N)/*Sal*I (L) digested destination vector (pETM6-4CL). *Nhe*I site was retained and can be reused for iterative assembly of downstream genes. Black box and arrow: T7 promoter and *lacO* operator; orange box: ribosome binding site; green box with arrow: open reading frame; red box: T7 terminator; *bla*: ampicillin resistance gene; *lacI*: lactose repressor gene; A: *Avr*II; X: *Xba*I; S: *Spe*I; N: *Nhe*I; and L: *Sal*I.

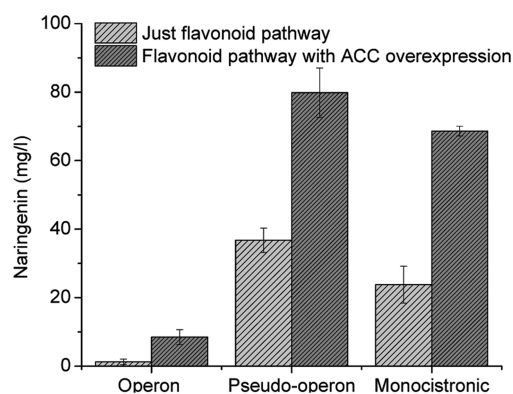


Figure 4. Impact of pathway configuration on the production potential of a three-gene flavonoid pathway in BL21*(DE3) growing in basic M9 media supplemented with *p*-coumaric acid as substrate at 30 °C.

but still followed the same pattern as the pathways without ACC overexpression, suggesting that intrinsic genetic configuration plays an important role in determining pathway output regardless of whether precursors are supplied.

Combinatorial Generation of Pathway Diversities.

While pathway configuration has a direct impact on the pathway output, other context-dependent genetic factors need to be considered when designing and optimizing a target metabolic pathway. One such genetic context is the order of the genes present in the pathway architecture. Studies have shown that rearrangement of gene order could lead to balanced turnover constant among investigated genes in a three-gene operon.⁴⁹ However, advanced gene assembly tools like overlap-PCR, SLIC, In-Fusion PCR (Clontech), and Gibson isothermal cloning are not sufficiently efficient in terms of rearranging gene order or configuration due to the predetermined fragment context specified by the overlap sequence.⁵⁰ Each of the

Table 2. Flavonoid Pathway Libraries Generated by ePathBricks-Directed Combinatorial Assembly^a

pETM6-Pc4CL- []PhCHS-[]MsCHI	pETM6-Pc4CL- []MsCHI-[]PhCHS	pETM6-PhCHS- []Pc4CL-[]MsCHI	pETM6-PhCHS- []MsCHI-[]Pc4CL	pETM6-MsCHI- []Pc4CL-[]PhCHS	pETM6-MsCHI- []PhCHS-[]Pc4CL
o, o	o, o	o, o	o, o	o, o	o, o
o, m	o, m	o, m	o, m	o, m	o, m
o, p	o, p	o, p	o, p	o, p	o, p
m, o	m, o	m, o	m, o	m, o	m, o
m, m	m, m	m, m	m, m	m, m	m, m
m, p	m, p	m, p	m, p	m, p	m, p
p, o	p, o	p, o	p, o	p, o	p, o
p, m	p, m	p, m	p, m	p, m	p, m
p, p	p, p	p, p	p, p	p, p	p, p

^aPc4CL, 4-coumaroyl-CoA ligase from *Petroselinum crispum*; PhCHS, chalcone synthase from *Petunia hybrida*; MsCHI, chalcone isomerase from *Medicago sativa*; o denotes the neighboring genes are organized in operon configuration; m denotes the neighboring genes are organized in monocistronic configuration; and p denotes the neighboring genes are organized in pseudo-operon or artificial operon configuration.

overlapping fragments is added through synthesized gene or customer-designed primers that overlap with the neighboring fragment, an approach that is not scalable for the construction of pathway libraries with variations in pathway configuration and gene order. For example, it would require 600 versions of primers or gene cassettes to assemble 10 overlapping DNA fragments in every possible arrangement and configuration. As a result, it is desirable to develop new tools adept at combinatorial assembly that would result in a library of possible pathway equivalents differing in pathway configuration and gene order.

Here we demonstrate that, with ePathBrick vectors, a three-gene flavonoid pathway library with 54 constructs could be efficiently assembled by three rounds of cloning in one week, when considering both pathway configuration and gene order (Table 2). Specifically, for the first round of cloning, 3 constructs with single pathway entities were assembled; for the second round of cloning, 18 constructs with double pathway entities were assembled based on the first round of cloning ($3C^1 \times 2C^1 \times 3 = 18$; note here double pathway entities could take six different orders out of the three gene pools and the second pathway entity could take three distinct configurations); for the third round of cloning, 54 constructs with triple pathway entities were assembled based on the second round of cloning (note here that the third pathway entity could take three distinct configuration). A detailed process about generation of pathway diversities is shown in Supplementary Table S3. Since all of the DNA manipulations are performed at the subcloning level, post-assembly sequence verification is optional and thereby the turnaround time for pathway assembly is greatly reduced and the whole process streamlined. By screening using double digestion, we successfully obtained all of the 54 constructs (Table 2) in one week, and representative digestion patterns of constructed pathways are shown in Figure 5 (digestion patterns for all of the 54 pathways can be found in Supplementary Figure S4). To our knowledge, ePathBrick vectors are the first synthetic biology tools that allow metabolic engineers to manipulate pathway configurations and generate pathway diversities at the individual gene level (subunit level), which would afford a promising approach in strain design and pathway optimization with practical applications in metabolic engineering.

Modular Assembly of Multigene Pathways on a Single ePathBrick Vector. The construction of multigene pathways and complex genetic circuits and redesign of existing biological systems require the precise and concerted assembly

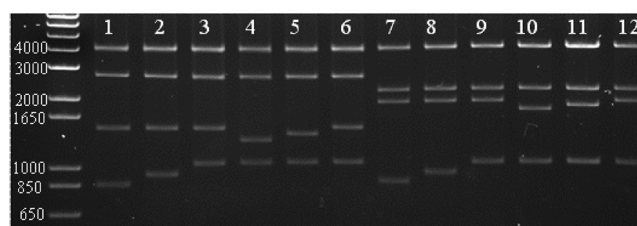


Figure 5. Representative digestion patterns of constructed flavanone pathway library. Ladder digestion pattern shows the operon, pseudo-operon, and monocistronic gene configuration. Pseudo-operon configurations are 80 bps more than operon configurations and monocistronic configurations are 96 bps more than pseudo-operon configurations. All plasmids were digested with *ApaI* and *KpnI*. Lane 0: 1 Kb plus ladder (bp); lane 1: pETM6-Pc4CL-mPhCHS-oMsCHI; lane 2: pETM6-Pc4CL-mPhCHS-pMsCHI; lane 3: pETM6-Pc4CL-mPhCHS-mMsCHI; lane 4: pETM6-Pc4CL-mMsCHI-oPhCHS; lane 5: pETM6-Pc4CL-mMsCHI-pPhCHS; lane 6: pETM6-Pc4CL-mMsCHI-mPhCHS; lane 7: pETM6-PhCHS-mPc4CL-oMsCHI; lane 8: pETM6-PhCHS-mPc4CL-pMsCHI; lane 9: pETM6-PhCHS-mPc4CL-mMsCHI; lane 10: pETM6-PhCHS-mMsCHI-oPc4CL; lane 11: pETM6-PhCHS-mMsCHI-pPc4CL; lane 12: pETM6-PhCHS-mMsCHI-mPc4CL. Digestion pattern for all 54 pathway constructs can be found in Supplementary Figure S4.

of multiple gene cassettes of various sizes.⁵¹ Sophisticated assembly tools based on yeast homologous recombination have been developed for assembling large DNA fragments encoding an entire biochemical pathway¹⁵ or iteratively integrating multigene pathways into yeast chromosome.⁵² Nevertheless, these tools are not amenable to *E. coli* cells due to the low recombination efficiency in most of the lab strains, and more importantly, current assembly tools are not flexible enough to support further modification of each of the expression cassette with elegantly designed regulatory control elements. From a pathway engineering perspective, it is of pressing importance to develop such tools that allow quick and reliable DNA assembly leading to programmable or predictable pathway output for strain optimization.

To demonstrate the applicability of the engineered ePathBrick vectors for rapid biosynthetic pathway assembly, a seven-gene recombinant pathway comprising the *E. coli* four-subunit acetyl-CoA carboxylase (encoded by *accA*, 960 bp; *accB*, 471 bp; *accC*, 1350 bp; and *accD*, 915 bp) and plant-derived three-gene flavonoid pathway (4 coumaroyl-CoA ligase *Pc4CL*, 1635 bp; chalcone synthase *PhCHS*, 1170 bp; and chalcone isomerase *MsCHI*, 669 bp) was assembled in pETM6

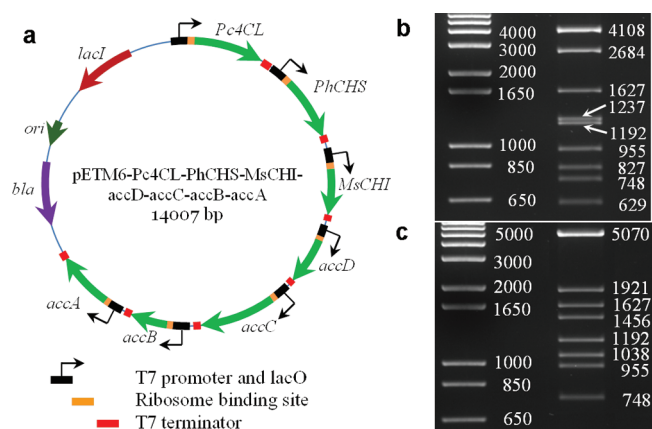


Figure 6. Efficient multigene pathway assembly on one single ePathBrick vector. (a) A seven-gene construct with plant-derived flavonoid pathway and *E. coli* four subunits acetyl-CoA carboxylase. *accA*, 960 bp; *accB*, 471 bp; *accC*, 1350 bp; and *accD*, 915 bp; *Pc4CL*, 4 coumaroyl-CoA ligase from *Petroselinum crispum*, 1635 bp; *PhCHS*, chalcone synthase from *Petunia hybrida*, 1170 bp; and *MsCHI*, chalcone isomerase from *Medicago sativa*, 669 bp. *bla*: ampicillin resistance gene; *lacI*: lactose repressor gene. (b) Digestion pattern for seven-gene construct pETM6-Pc4CL-PhCHS-MsCHI-accDCBA with *ApaI* and *XhoI*. First lane, 1 Kb plus ladder; second lane, digested plasmid (note CHS gene contains an intergenic *XhoI* site). (c) Digestion pattern for seven-gene construct pETM6-Pc4CL-PhCHS-MsCHI-accDCBA with *ApaI* and *NdeI*. First lane, 1 Kb plus ladder; second lane, digested plasmid. Supplementary Figure S5 contains a detailed plasmid map with labeled restriction sites.

vector (Figure 6a). Assembly of this seven-gene pathway (~9 Kb including regulatory region) required three rounds of cloning in one week, and intermediary subpathway constructs such as pETM6-*Pc4CL-PhCHS-MsCHI* and pETM6-*accD-accC-accB-accA* were assembled in parallel, thus greatly increasing the assembly efficiency. Elegantly selected restriction enzymes were used to verify the final construct, and the digested plasmid showed the correct fragment pattern (Figure 6b and c). Plasmids isolated from five out of seven randomly picked colonies were positive constructs, representing more than 70% assembly efficiency, which is comparable to the efficiency reported in yeast when using the homologous recombination-based DNA assembler method.¹⁵ Tested in the Bl21*(DE3) strain, this seven-gene pathway led to a slightly lower flavonoid production (61.2 mg/L) compared with the strain carrying individual flavonoid biosynthetic pathway encoding genes and acetyl-CoA carboxylase encoding genes on two separate vectors (68.6 mg/L, Figure 4), suggesting that this seven-gene pathway was functional.

Summary and Conclusions. As the cost of commercial synthesis of genes is declining, our ability to physically construct complex biological devices/pathways from basic

DNA parts is becoming a limiting factor in implementing the vision of synthetic biology. Though past decades' advancement in synthetic biology has led to a variety of strategies to tackle DNA constructs, a robust platform specifically for metabolic pathway construction and optimization has yet to be developed. Here we present the development of a set of standard vectors customized for modular pathway design and optimization. The engineered ePathBrick vectors extend the BioBrick paradigm in terms of part reuse and standardization. By strategically engineering four isocaudamer pairs (*AvrII*, *XbaI*, *SpeI*, and *NheI*) into Novagen Duet vectors, the resultant ePathBrick vectors encompass several unique features allowing for tunable transcription output, combinatorial generation of pathway diversities, and modular assembly of multigene pathways (~9 Kb on one vector). In addition, ePathBricks have retained the major advantages of the original Duet vectors (Table 3), such as versatility in promoter strength and plasmid copy number, compatible replication origin, and independent antibiotic marker. Since four compatible plasmids can be used simultaneously, it is estimated that a pathway of 36 Kb total size can be easily assembled, which is sufficient for expressing a typical secondary metabolic pathway.

Perhaps the most prominent feature for the engineered ePathBrick vector is that expression cassettes and individual regulatory elements such as promoter, operator, ribosome binding sites, and terminators can be combinatorially swapped and rearranged in any order and any configuration. Indeed, combinatorial transcription control through modification of the regulatory element has offered tremendous opportunities for fine-tuning gene expression and generating digital-like genetic circuits.^{22,44} With ePathBrick vectors, hybrid promoters with complex regulatory architecture can be easily composed through iterative incorporation of transcriptional activation or repression signals, representing a powerful tool for coordinating gene expression among the investigated pathways. Another challenge faced by synthetic biologists is the ability to combinatorially generate pathway diversities.⁵⁰ As an attempt to address this challenge, a three-gene flavonoid pathway with three distinct configurations was successfully constructed and further diversified to 54 pathway equivalents differing in pathway configuration and gene order; coupled with high-throughput screening techniques, we envision that this combinatorial strategy would greatly improve our ability to exploit the full potential of microbial cell factories for recombinant metabolite production.

In light of the past two decades' achievements, metabolic engineering has remained a collection of elegant demonstrations instead of becoming a state-of-the-art discipline. The primary reason behind this dilemma is that many of the tools adopted for pathway engineering are only specific to certain pathways or hosts.⁵³ An ambitious goal for a synthetic biologist

Table 3. Major Features of ePathBrick Vectors

vector name	promoter	promoter strength ^a	size (bp)	replication origin	resistance marker	antibiotic ($\mu\text{g/mL}$)
pETM6	T7	1.00	5203	ColE1	ampicillin	80
pCDM4	T7	0.38	3810	CloDF13	streptomycin	50
pACM4	T7	0.29	3956	P15A	chloramphenicol	25
PCOM4	T7	0.14	3667	CoLA	kanamycin	50
pRSM3	T7	0.52	3777	RSF1030	kanamycin	50

^aPromoter strength reported here is the relative promoter activity compared to pETM6. Full sequence for each vector in Genbank format can be found in the Supporting Information.

is to develop generalizable tools and techniques that are universally applicable to all microbial hosts and pathways. Central to this endeavor is an approach called “multivariate modular metabolic engineering” (MMME), which aims at debottlenecking pathway limitations and optimizing a pathway’s potential through systematic investigation of pathway input variables. Several excellent examples, such as tuning promoter strength and plasmid copy numbers, have been presented for optimizing the biosynthesis of important metabolites, such as taxol¹² and artemisinin¹³ precursors. However, the whole engineering process associated with the MMME optimization is tedious and time-consuming as it usually involves the assembly of several dozens of pathway constructs for a small-scale pathway (<10 genes). With ePathBrick vectors, the process of pathway construction is streamlined and thus the assembly efficiency can be greatly increased. It is important to note here that delicately designed statistical experiments can be used to screen main effects for identifying pathway limitations instead of performing a full factorial experiment. Pathway performance can be directly tested on the basis of sophisticated statistical design. Combined with synthetic promoter libraries⁵⁴ or synthetic ribosome binding sites,⁹ the ePathBrick vectors provide a robust tool for rapid design, construction, and optimization of multigene pathways in *E. coli*. Taken together, the ePathBrick vectors presented here provide a flexible platform for engineering metabolic pathways in *E. coli* with a variety of applications in biofuels, fine chemicals, and pharmaceuticals production.

METHODS

ePathBrick Vectors Construction. Plasmid construction and DNA manipulations were performed following standard molecular cloning protocols. Strains and plasmids used in this study are listed in Supplementary Table S1. All PCR primers used for site-directed mutagenesis and gene amplification are listed in Supplementary Table S2. Plasmid maintenance and propagation were performed using *E. coli* DH5 α strain. Site-directed mutagenesis was performed in *E. coli* BW27784 using QuikChange II Site-Directed Mutagenesis Kits from Agilent. The five duet vectors pET-Duet, pCDF-Duet, pACYC-Duet, pCoLA-Duet, and pRSF-Duet were purchased from Novagen. Seven rounds of DNA manipulations were performed in order to create pETM6. Specifically, *NdeI* was inserted before *NcoI* on pET-Duet resulting in plasmid pETM0 using site-directed (SD) primers *Nde_IF* and *Nde_IR*. Next, the *NdeI* digested pETM0 was self-ligated (note here pETM0 contains two *NdeI* sites) to excise multicloning site I resulting in plasmid pETM1. The *AvrII* site on pETM1 was eliminated to give pETM2 using SD primers *Avr_RF* and *Avr_RR*. The *NheI* site was inserted after the T7 terminator on pETM2 to give pETM3 using SD primers *Nhe_IF* and *Nhe_IR*. The *Sall* site was inserted between the *NheI* site and *f1* origin on pETM3 to give pEM4 using SD primers *Sal_IF* and *Sal_IR*. The *AvrII* site was inserted before the T7 promoter on pETM4 to give pETM5 using SD primers *Avr_IF* and *Avr_IR*. Finally, the *SpeI* site was inserted into pETM5 to give pETM6 using SD primers *Spe_IF* and *Spe_IR*. To create pCDM4, the native *NheI* site on pCDF-Duet was eliminated to give pCDM1 using SD primers *Nhe_CdF* and *Nhe_CdR*. The *Sall* site was inserted after the T7 terminator on pCDM1 to give pCDM2 using SD primers *Sal_CdF* and *Sal_CdR*. An *ApaI-Sall* digested fragment from pETM5 was ligated into *ApaI-Sall* digested pCDM2 to give pCDM3. An *ApaI-Sall* digested fragment from pETM6 was

ligated into *ApaI-Sall* digested pCDM2 to give pCDM4. The construction of pACM4, pCOM4, and pRSM3 is described in detail in the Supporting Information. All clones were screened by restriction digestion analysis and verified by gene sequencing.

Reporter Plasmid Construction. A randomly chosen upstream activation sequence⁴³ (UAS) attached with eGFP was synthesized by Integrated DNA Technologies (IDT). Detailed sequence and gene context information is provided in supplementary Figure S3. eGFP was PCR amplified from pIDTBlue-UAS-eGFP using primers eGFP_NdeF and eGFP_KpnR. Next, *NdeI/KpnI* digested PCR products were inserted into the *NdeI* and *KpnI* site of pETM6, pCDM4, pACM4, pCOM4 and pRSM3 to give construct pETM6-eGFP, pCDM4-eGFP, pACM4-eGFP, pCOM4-eGFP and pRSM3-eGFP, respectively. To incorporate UAS into the regulatory region of pETM6, UAS-eGFP fragment was PCR amplified from pIDTBlue-UAS-eGFP using primer pairs UAS_NheF and eGFP_KpnR. Next, *NheI/KpnI* digested PCR products were inserted to the *XbaI/KpnI* site of pETM6 to give pETM6-1X[UAS]-eGFP. The original *XbaI* site on pETM6 was destroyed upon *XbaI* and *NheI* ligation and the resulting pETM6-1X[UAS]-eGFP contains another copy of *XbaI*, which can be used for iterative integration of multiple copies of UAS in a tandem manner. For incorporation of additional copies of *lacO* into the regulatory region, detailed experimental procedures are provided in Supporting Information. All clones were screened by restriction digestion analysis and verified by gene sequencing.

Assay of Gene Expression. Fluorescence signal intensity was used to characterize the promoter activity among the engineered ePathBrick vectors. Host cell BL21*(DE3) transformed with reporter plasmids was grown overnight in LB at 37 °C, 250 rpm. The next morning, 10 mL of fresh LB was inoculated with 8% (v/v) overnight culture in 50-mL Corning tubes and grown at 37 °C, 250 rpm for approximately 2.5 h (OD of 0.4 in 96-well plate). Subsequently, 240 μ L of cell culture was transferred to Greiner Bio-one 96-well fluorescence plate (Bio-Greiner, chimney black, flat clear bottom) with an Eppendorf multichannel pipet. At the same time, 10 μ L of stock IPTG solution was added to make a gradient concentration ranging from 1/16 μ M to 1 mM. Fluorescence plate was covered and sealed with parafilm to prevent any volume loss due to evaporation. Cells in fluorescence plate were grown at 30 °C with shaking at 220 rpm on a benchtop plate shaker (Labnet VorTemp 56 shaker incubator). Cell optical density and expression of green fluorescence protein were simultaneously detected every 30–45 min using a Biotek Synergy 4 microplate reader. Optical density was read at 600 nm, and the excitation and emission wavelengths for eGFP were set at 485 \pm 20 and 528 \pm 20 nm, respectively. All experiments were performed in triplicates.

Flavanone Pathway Assembly. 4-Coumaroyl-CoA ligase (4CL), chalcone synthase (CHS), and chalcone isomerase (CHI) gene fragments were PCR amplified from either pET-PhCHS-MsCHI or pCDF-4CL³⁶ using primer pairs 4CL_NdeF/4CL_KpnR, CHS_NdeF/CHS_KpnR, and CHI_NdeF/CHI_KpnR, respectively. *NdeI/KpnI* digested PCR fragments were cloned into the *NdeI* and *KpnI* site of pETM6 to give constructs pETM6-Pc4CL, pETM6-PhCHS, and pETM6-MsCHI, respectively. *SpeI* site within CHS was silently mutated by site-directed mutagenesis with primer pairs CHS_SpeF and CHS_SpeR, allowing for the built-in *SpeI* site to be unique and

be used for the future assembly step. *accA*, *accB*, and *accC* gene fragments were PCR amplified from plasmid pMSD8 provided by Prof. Cronan⁵⁵ using primer pairs *AccA_NdeF/AccA_XhoR*, *AccB_NdeF/AccB_XhoR*, and *AccC_NdeF/AccC_XhoR*, respectively. *accD* fragment was PCR amplified from *E. coli* K-12 genomic DNA (prepared by Purelink genomic DNA kits) using primer pair *AccD_NdeF/AccD_XhoR*. *NdeI/XhoI* digested PCR fragments were cloned into the *NdeI* and *XhoI* site of pETM6 to give constructs pETM6-*accA*, pETM6-*accB*, pETM6-*accC*, and pETM6-*accD* respectively. Gene assembly was performed based on these individual constructs. Briefly, operon configuration was achieved by ligating the *XbaI/SalI* digested donor construct with the *SpeI/SalI* digested receiver construct; pseudo-operon configuration was achieved by ligating the *AvrII/SalI* digested donor construct with the *SpeI/SalI* digested receiver construct; monocistronic configuration was achieved by ligating the *AvrII/SalI* digested donor construct with the *NheI/SalI* digested receiver construct. Multifragment assembly can be performed in parallel and in rare cases, high affinity *ApaI* site on *lacI* gene was used (instead of *SalI*) to improve ligation efficiency.

Flavanone Fermentation and Analysis. Flavanone production was performed based on a two-step fermentation protocol.³⁵ Overnight cultures were used to inoculate 40 mL of fresh LB supplemented with 0.2% glucose at 37 °C with shaking at 300 rpm. Heterologous gene expression was induced during the midexponential phase (approximately OD 0.6–0.8) by addition of 1 mM IPTG, and the cultures were allowed to grow at 30 °C for an additional 6–8 h. After induction, the bacterial pellet was harvested by centrifugation and suspended with 16 mL of M9 modified medium (1 × M9 salts, 8 g/L glucose, 1 mM MgSO₄, 0.1 mM CaCl₂, 6 μM biotin, 10 nM thiamine, 2.6 mM *p*-coumaric acid, 1 mM IPTG). Fermentation was performed in 250-mL flasks with orbital shaking at 300 rpm and 30 °C. Flavanones were extracted with 50% ethanol after 24 h of fermentation, then the *E. coli* pellet was removed by centrifugation (14,000 rpm for 5 min), and the supernatant was analyzed for flavanone quantification. Flavanones were analyzed by the Agilent 1260 HPLC system equipped with a ZORBAX SB-C18 column (5 μm, 4.6 × 150 mm) kept at 25 °C and a diode array detector (DAD). The mobile phase contained 35% acetonitrile (with 0.1% formic acid) and 65% water (with 0.1% formic acid). The retention time for *p*-coumaric acid and naringenin were around 1.9 and 5 min, respectively. All experiments were performed in triplets.

■ ASSOCIATED CONTENT

■ Supporting Information

Detailed sequence information of ePathBrick vectors in Genbank format. This material is available free of charge via the Internet at <http://pubs.acs.org>.

■ AUTHOR INFORMATION

Corresponding Author

*E-mail: koffam@rpi.edu.

Author Contributions

P.X. and M.A.G.K. conceived the study and designed the experiments; P.X. performed the experiments with input from A.V.; N.B., P.X., and M.A.G.K. prepared the manuscript; and all authors contributed to the discussion of the research and interpretation of data.

Notes

The authors declare the following competing financial interest(s): A provisional patent that is based on the results presented here has been filed by Office of Technology Commercialization, Rensselaer Polytechnic Institute (Case no. 1470). A.V. and N.B. declare no competing financial interests.

■ ACKNOWLEDGMENTS

We thank Prof. Wenya Wang and Brady Cress for their inspiring discussion and advice on this work. We would like to acknowledge Prof. Cronan at University of Illinois for providing the pMSD8 construct. This work was supported by startup funds and Biocatalysis Constellation funds awarded to M.A.G.K. by Rensselaer Polytechnic Institute.

■ REFERENCES

- (1) Peralta-Yahya, P. P., Ouellet, M., Chan, R., Mukhopadhyay, A., Keasling, J. D., and Lee, T. S. (2011) Identification and microbial production of a terpene-based advanced biofuel. *Nat. Commun.* 2, 483.
- (2) Wargacki, A. J., Leonard, E., Win, M. N., Regitsky, D. D., Santos, C. N., Kim, P. B., Cooper, S. R., Raisner, R. M., Herman, A., Sivitz, A. B., Lakshmanaswamy, A., Kashiyama, Y., Baker, D., and Yoshikuni, Y. (2012) An engineered microbial platform for direct biofuel production from brown macroalgae. *Science* 335, 308–313.
- (3) Xu, P., and Koffas, M. A. G. (2010) Metabolic engineering of *Escherichia coli* for biofuel production. *Biofuels* 1, 493–504.
- (4) Westfall, P. J., Pitera, D. J., Lenihan, J. R., Eng, D., Woolard, F. X., Regentin, R., Horning, T., Tsuruta, H., Melis, D. J., Owens, A., Fickes, S., Diola, D., Benjamin, K. R., Keasling, J. D., Leavell, M. D., McPhee, D. J., Renninger, N. S., Newman, J. D., and Paddon, C. J. (2012) Production of amorphadiene in yeast, and its conversion to dihydroartemisinin acid, precursor to the antimalarial agent artemisinin. *Proc. Natl. Acad. Sci. U.S.A.* 109, E1111–E1118.
- (5) Zhou, Y. J., Gao, W., Rong, Q., Jin, G., Chu, H., Liu, W., Yang, W., Zhu, Z., Li, G., Zhu, G., Huang, L., and Zhao, Z. K. (2012) Modular pathway engineering of diterpenoid synthases and the mevalonic acid pathway for miltiradiene production. *J. Am. Chem. Soc.* 134, 3234–3241.
- (6) Cox, R., Surette, M., and Elowitz, M. (2007) Programming gene expression with combinatorial promoters. *Mol. Syst. Biol.* 3, 145.
- (7) Blazeck, J., Liu, L., Redden, H., and Alper, H. (2011) Tuning gene expression in *Yarrowia lipolytica* by a hybrid promoter approach. *Appl. Environ. Microbiol.* 77, 7905–7914.
- (8) Michener, J. K., Thodey, K., Liang, J. C., and Smolke, C. D. (2011) Applications of genetically-encoded biosensors for the construction and control of biosynthetic pathways. *Metab. Eng.* 14, 212–222.
- (9) Salis, H., Mirsky, E., and Voigt, C. (2009) Automated design of synthetic ribosome binding sites to control protein expression. *Nat. Biotechnol.* 27, 946–950.
- (10) Dueber, J., Wu, G., Malmirchegini, G., Moon, T., Petzold, C., Ullal, A., Prather, K., and Keasling, J. (2009) Synthetic protein scaffolds provide modular control over metabolic flux. *Nat. Biotechnol.* 27, 753–759.
- (11) Juminaga, D., Baidoo, E. E., Redding-Johanson, A. M., Batth, T. S., Burd, H., Mukhopadhyay, A., Petzold, C. J., and Keasling, J. D. (2012) Modular engineering of L-tyrosine production in *Escherichia coli*. *Appl. Environ. Microbiol.* 78, 89–98.
- (12) Ajikumar, P., Xiao, W., Tyo, K., Wang, Y., Simeon, F., Leonard, E., Mucha, O., Phon, T., Pfeifer, B., and Stephanopoulos, G. (2010) Isoprenoid pathway optimization for taxol precursor overproduction in *Escherichia coli*. *Science* 330, 70–74.
- (13) Anthony, J., Anthony, L., Nowroozi, F., Kwon, G., Newman, J., and Keasling, J. (2009) Optimization of the mevalonate-based isoprenoid biosynthetic pathway in *Escherichia coli* for production of the anti-malarial drug precursor amorpha-4,11-diene. *Metab. Eng.* 11, 13–19.

- (14) Bokinsky, G., Peralta-Yahya, P. P., George, A., Holmes, B. M., Steen, E. J., Dietrich, J., Soon Lee, T., Tullman-Ercek, D., Voigt, C. A., Simmons, B. A., and Keasling, J. D. (2011) Synthesis of three advanced biofuels from ionic liquid-pretreated switchgrass using engineered *Escherichia coli*. *Proc. Natl. Acad. Sci. U.S.A.* 108, 19949–19954.
- (15) Shao, Z., and Zhao, H. (2009) DNA assembler, an *in vivo* genetic method for rapid construction of biochemical pathways. *Nucleic Acids Res.* 37, e16.
- (16) Shao, Z., Luo, Y., and Zhao, H. (2011) Rapid characterization and engineering of natural product biosynthetic pathways via DNA assembler. *Mol. Biosyst.* 7, 1056–1059.
- (17) Li, M. Z., and Elledge, S. J. (2007) Harnessing homologous recombination *in vitro* to generate recombinant DNA via SLIC. *Nat. Methods* 4, 251–256.
- (18) Gibson, D. G., Young, L., Chuang, R. Y., Venter, J. C., Hutchison, C. A., and Smith, H. O. (2009) Enzymatic assembly of DNA molecules up to several hundred kilobases. *Nat. Methods* 6, 343–345.
- (19) Lee, T. S., Krupa, R. A., Zhang, F., Hajimorad, M., Holtz, W. J., Prasad, N., Lee, S. K., and Keasling, J. D. (2011) BglBrick vectors and datasheets: A synthetic biology platform for gene expression. *J. Biol. Eng.* 5, 12.
- (20) Liang, X., Peng, L., Tsvetanova, B., Li, K., Yang, J. P., Ho, T., Shirley, J., Xu, L., Potter, J., Kudlicki, W., Peterson, T., and Katzen, F. (2012) Recombination-based DNA assembly and mutagenesis methods for metabolic engineering. *Methods Mol. Biol.* 834, 93–109.
- (21) Vick, J. E., Johnson, E. T., Choudhary, S., Bloch, S. E., Lopez-Gallego, F., Srivastava, P., Tikh, I. B., Wawrzyn, G. T., and Schmidt-Dannert, C. (2011) Optimized compatible set of BioBrick vectors for metabolic pathway engineering. *Appl. Microbiol. Biotechnol.* 92, 1275–1286.
- (22) Ayukawa, S., Kobayashi, A., Nakashima, Y., Takagi, H., Hamada, S., Uchiyama, M., Yugi, K., Murata, S., Sakakibara, Y., Hagiya, M., Yamamura, M., and Kiga, D. (2010) Construction of a genetic AND gate under a new standard for assembly of genetic parts. *BMC Genomics* 11 (Suppl 4), S16.
- (23) Norville, J. E., Derda, R., Gupta, S., Drinkwater, K. A., Belcher, A. M., Leschziner, A. E., and Knight, T. F. (2010) Introduction of customized inserts for streamlined assembly and optimization of BioBrick synthetic genetic circuits. *J. Biol. Eng.* 4, 17.
- (24) Knight, T. (2003) Idempotent Vector Design for Standard Assembly of Biobricks, MIT Synthetic Biology Working Group. <http://web.mit.edu/synbio/release/docs/biobricks.pdf>.
- (25) Canton, B., Labno, A., and Endy, D. (2008) Refinement and standardization of synthetic biological parts and devices. *Nat. Biotechnol.* 26, 787–793.
- (26) Shetty, R. P., Endy, D., and Knight, T. F. (2008) Engineering BioBrick vectors from BioBrick parts. *J. Biol. Eng.* 2, 5.
- (27) Anderson, J. C., Dueber, J. E., Leguia, M., Wu, G. C., Goler, J. A., Arkin, A. P., and Keasling, J. D. (2010) BglBricks: A flexible standard for biological part assembly. *J. Biol. Eng.* 4, 1.
- (28) Atsumi, S., Hanai, T., and Liao, J. (2008) Non-fermentative pathways for synthesis of branched-chain higher alcohols as biofuels. *Nature* 451, 86–89.
- (29) Shen, C., Lan, E., Dekishima, Y., Baez, A., Cho, K., and Liao, J. (2011) Driving forces enable high-titer anaerobic 1-butanol synthesis in *Escherichia coli*. *Appl. Environ. Microbiol.* 77, 2905–2915.
- (30) Tsuruta, H., Paddon, C. J., Eng, D., Lenihan, J. R., Horning, T., Anthony, L. C., Regentin, R., Keasling, J. D., Renninger, N. S., and Newman, J. D. (2009) High-level production of amorpha-4,11-diene, a precursor of the antimalarial agent artemisinin, in *Escherichia coli*. *PLoS One* 4, e4489.
- (31) Tolia, N. H., and Joshua-Tor, L. (2006) Strategies for protein coexpression in *Escherichia coli*. *Nat. Methods* 3, 55–64.
- (32) Tseng, H. C., Martin, C. H., Nielsen, D. R., and Prather, K. L. (2009) Metabolic engineering of *Escherichia coli* for enhanced production of (R)- and (S)-3-hydroxybutyrate. *Appl. Environ. Microbiol.* 75, 3137–3145.
- (33) Nawabi, P., Bauer, S., Kyrpides, N., and Lykidis, A. (2011) Engineering *Escherichia coli* for biodiesel production utilizing a bacterial fatty acid methyltransferase. *Appl. Environ. Microbiol.* 77, 8052–8061.
- (34) Nielsen, D. R., Leonard, E., Yoon, S. H., Tseng, H. C., Yuan, C., and Prather, K. L. (2009) Engineering alternative butanol production platforms in heterologous bacteria. *Metab. Eng.* 11, 262–273.
- (35) Xu, P., Ranganathan, S., Fowler, Z., Maranas, C., and Koffas, M. (2011) Genome-scale metabolic network modeling results in minimal interventions that cooperatively force carbon flux towards malonyl-CoA. *Metab. Eng.* 13, 578–587.
- (36) Leonard, E., Lim, K., Saw, P., and Koffas, M. (2007) Engineering central metabolic pathways for high-level flavonoid production in *Escherichia coli*. *Appl. Environ. Microbiol.* 73, 3877–3886.
- (37) Morrone, D., Lowry, L., Determan, M. K., Hershey, D. M., Xu, M., and Peters, R. J. (2010) Increasing diterpene yield with a modular metabolic engineering system in *E. coli*: comparison of MEV and MEP isoprenoid precursor pathway engineering. *Appl. Microbiol. Biotechnol.* 85, 1893–1906.
- (38) Zha, W., Rubin-Pitel, S. B., Shao, Z., and Zhao, H. (2009) Improving cellular malonyl-CoA level in *Escherichia coli* via metabolic engineering. *Metab. Eng.* 11, 192–198.
- (39) Andrianantoandro, E., Basu, S., Karig, D. K., and Weiss, R. (2006) Synthetic biology: new engineering rules for an emerging discipline. *Mol. Syst. Biol.* 2, 2006.0028.
- (40) Crook, N. C., Freeman, E. S., and Alper, H. S. (2011) Re-engineering multicloning sites for function and convenience. *Nucleic Acids Res.* 39, e92.
- (41) Kroll, J., Steinle, A., Reichelt, R., Ewering, C., and Steinbüchel, A. (2009) Establishment of a novel anabolism-based addition system with an artificially introduced mevalonate pathway: complete stabilization of plasmids as universal application in white biotechnology. *Metab. Eng.* 11, 168–177.
- (42) Hartner, F., Ruth, C., Langenegger, D., Johnson, S., Hyka, P., Lin-Cereghino, G., Lin-Cereghino, J., Kovar, K., Cregg, J., and Glieder, A. (2008) Promoter library designed for fine-tuned gene expression in *Pichia pastoris*. *Nucleic Acids Res.* 36, e76.
- (43) Schujman, G., Guerin, M., Buschiazzo, A., Schaeffer, F., Llarrull, L., Reh, G., Vila, A., Alzari, P., and de Mendoza, D. (2006) Structural basis of lipid biosynthesis regulation in Gram-positive bacteria. *EMBO J.* 25, 4074–4083.
- (44) Wang, B., Kitney, R., Joly, N., and Buck, M. (2011) Engineering modular and orthogonal genetic logic gates for robust digital-like synthetic biology. *Nat. Commun.* 2, 508.
- (45) Kuhlman, T., Zhang, Z., Saier, M. H., and Hwa, T. (2007) Combinatorial transcriptional control of the lactose operon of *Escherichia coli*. *Proc. Natl. Acad. Sci. U.S.A.* 104, 6043–6048.
- (46) Okuda, S., Kawashima, S., Kobayashi, K., Ogasawara, N., Kanehisa, M., and Goto, S. (2007) Characterization of relationships between transcriptional units and operon structures in *Bacillus subtilis* and *Escherichia coli*. *BMC Genomics* 8, 48.
- (47) Lim, H., Lee, Y., and Hussein, R. (2011) Fundamental relationship between operon organization and gene expression. *Proc. Natl. Acad. Sci. U.S.A.* 108, 10626–10631.
- (48) Lim, C., Fowler, Z., Hueller, T., Schaffer, S., and Koffas, M. (2011) High-Yield Resveratrol Production in Engineered *Escherichia coli*. *Appl. Environ. Microbiol.* 77, 3451–3460.
- (49) Hiroe, A., Tsuge, K., Nomura, C. T., Itaya, M., and Tsuge, T. (2012) Rearrangement of gene order in the phaCAB operon leads to effective production of ultra-high-molecular-weight poly[(R)-3-hydroxybutyrate] in genetically engineered *Escherichia coli*. *Appl. Environ. Microbiol.* 78, 3177–3184.
- (50) Ellis, T., Adie, T., and Baldwin, G. S. (2011) DNA assembly for synthetic biology: from parts to pathways and beyond. *Integr. Biol. (Camb.)* 3, 109–118.
- (51) Tsvetanova, B., Peng, L., Liang, X., Li, K., Yang, J. P., Ho, T., Shirley, J., Xu, L., Potter, J., Kudlicki, W., Peterson, T., and Katzen, F. (2011) Genetic assembly tools for synthetic biology. *Methods Enzymol.* 498, 327–348.

(52) Wingler, L. M., and Cornish, V. W. (2011) Reiterative Recombination for the *in vivo* assembly of libraries of multigene pathways. *Proc. Natl. Acad. Sci. U.S.A.* 108, 15135–15140.

(53) Yadav, V. G., De Mey, M., Giaw Lim, C., Kumaran Ajikumar, P., and Stephanopoulos, G. (2012) The future of metabolic engineering and synthetic biology: Towards a systematic practice. *Metab. Eng.* 14, 223–241.

(54) Alper, H., Fischer, C., Nevoigt, E., and Stephanopoulos, G. (2005) Tuning genetic control through promoter engineering. *Proc. Natl. Acad. Sci. U.S.A.* 102, 12678–12683.

(55) Davis, M. S., Solbiati, J., and Cronan, J. E. (2000) Overproduction of acetyl-CoA carboxylase activity increases the rate of fatty acid biosynthesis in *Escherichia coli*. *J. Biol. Chem.* 275, 28593–28598.